

Jeng-Haur Horng

Chair-Professor
Department of Power Mechanical
Engineering
National Formosa University
Taiwan, ROC

Dipto Biswas

Research Assistant
Department of Power Mechanical
Engineering
National Formosa University
Taiwan, ROC

Adhitya

Research Assistant
Department of Power Mechanical
Engineering
National Formosa University
Taiwan, ROC

Qumrul Ahsan

Professor
Department of Mechanical and Production
Engineering
Ahsanullah University of Science and
Technology, Dhaka
Bangladesh

Investigation of Running-in Process Based on Surface Roughness Parameters, Real Contact Area Ratio and Tribological Properties

The running-in process is the initial process for the new moving parts wearing against each other to establish the shape adjustment that will regulate them into a stable relationship for the rest of their working life. The objective of this research is to investigate and evaluate the running-in process by using disk-on-block line contact device. Due to its empirical nature and well-ploughed analysis, an asperity micro-contact model is considered. The experiment is performed by varying the surface roughness of the block with rigid smooth sphere surface under specific condition. The effects of surface roughness, load, speed, and lubrication on the running-in behaviour is studied. The running-in process encourage plastic deformation of asperities and created microstructural changes on contact surfaces. The theoretical and experiment result shows that the plasticity index ψ , surface roughness parameter β , real contact area ratio A_0^ and specific film thickness λ is influenced by the running-in process.*

Keywords: Running-in process, surface roughness parameter, real contact area, specific film thickness, plasticity index, stribeck curve.

1. INTRODUCTION

In general, running-in refers to the mechanism during the initial level of usage by which contacting machine parts improve in conformity, surface topography, and frictional behaviour [1]. In the UK, term "running-in" is more widely used than in America, where "break-in" or "wear-in" are favoured. During the initial period of surface contact, a lot of changes in the sliding or rolling contacting surfaces, asperity contact surface zones, and interfacial species such as lubricants or wear particles occur. When freshly prepared, unworn surfaces come in the contact with one another, or when a worn part on one side of a couple is replaced with a new one, modifications occur. Researchers have shown that applying a running-in process to certain tribology components will result in better operating performance. Khonsari et al. [2] examines published research on the topic of running-in and displays each paper's remarks. Running-in studies have been conducted for many years; nevertheless, because of the intricacy of the phenomenon, many issues have arisen that have yet to be resolved. For some engineering applications, the basic reasons why a running-in procedure can improve performance are better understood than for others; however, depending on the tribology system and materials involved, the following modifications have all been related with running-in. When two surfaces collide, contact can occur at just a few points at first to support the normal load. When the normal load is increased, the

surfaces move closer together, more high asperities on the two surfaces come into interaction, and existing contacts expand to support the increased load [3]. Some asperities are elastically deformed in most contact situations, while others are plastically deformed. Geometrical changes in surface, contact areas and contact depths can be calculated using the theory of interaction between elastic bodies.

The quality of running-in process depends on the suitable selection of the factors that affect the running in process. Basically, in contact body, running-in influenced by the surface topography, load, speed, friction, time and lubricants. If there are no visible defects from the manufacturing process, surface roughness is the significant factor that mostly affects the run-in. The impact of the initial surface topography on running-in results has been studied by a number of researchers. Hansen et al. [4] developed a 3D surface re-location approach and explored topographic transformations of rolling-sliding in running-in under non-conformal EHL contacts empirically. To research the impact of surface topography during running-in, the majority of the researchers considers one surface to be relatively smooth and hard running against a deformable rough flat surface. Surface roughness with a transversely line up pattern has higher friction than roughness pattern with other orientations like longitudinal because the asperities orientation on surfaces with transverse patterns obstructs the fluid film and induces further asperity–asperity interaction [5]. Tribological behaviour of textured surfaces and smooth surfaces under different lubrication condition is investigated by Nikolakopoulos et al. [6] using a block on ring test apparatus. Experimental results shows that textured surface improved the wear resistance and better lubricant distribution on the surface due to the less friction. The plasticity index

Received: June 2021, Accepted: August 2021

Correspondence to: Jeng-Haur Horng
Department of Power Mechanical Engineering,
National Formosa University, Taiwan, ROC
E-mail: jhhorng@gmail.com

doi:10.5937/fme2104988H

© Faculty of Mechanical Engineering, Belgrade. Allrights reserved

FME Transactions (2021) 49, 988-996 988

also used to determine the impact of surface topography during run-in and it increases with the increase in surface roughness and sliding speed [7]. Running-in is accomplished by gradually increasing the load and velocity. The consistency of a run-in surface improves by rising the contact pressure to a level that does not exceed a critical contact pressure. Increased contact pressure above the critical value causes extreme wear. Wang [8] also addresses the smoothing of rough surfaces by increasing the load. Surface roughness after running-in decreases as the applied load increases. Vite-Torres et al. [9], studied the wear and corrosion characteristics of nickel coating on carbon steel and shows that coated surface gives less wear and better corrosion resistance on the surface.

The existence of lubricants and additives has a major impact on the change in micro-geometry during running-in under unchanged contact conditions. Parlar et al. [10] experimentally studied the friction coefficient and wear loss of MnP/Austempered coated cast iron against crankshaft for dry and boundary lubrication and found that austempered coated cast iron gives better result than Mnp coated cast iron on boundary lubrication but Mnp coated show better results in dry lubrication. The surface tribological parameters of the circulation lubricant were evaluated by Ta et al. [11] in the presence and absence of the running-in process, as well as with varied ZDDP concentrations added to the lubricant. Function of lubrication are to dissipate heat produced inside the machine as a result of friction and other factors, to have a proper oil film on the rolling contact surface in order to extend machine fatigue life, to avoid dirt pollution and corrosion. While lubricant has a major impact on reducing running-in time, careful selection is needed to achieve the best results for the running-in method. The impact of running-in and tribofilms on gear failures and friction was studied by Ziegltrum et al. [12], and the results revealed that during running-in, tribofilm production can be more important than surface roughness change in terms of gear failures and friction. The central film thickness for electrohydro-dynamic lubrication was investigated by Dowson et al. [13] and showed for the first time full numerical film thickness and pressure distributions and a curve fitted minimum film prediction.

Running-in is a technique for synchronizing two contacting components in a rolling or sliding situation. Many parameters changed during the running-in process. The aim of the research is to investigate the different effect of tribological parameters for the running-in application. The line contact experiment is used in this analysis to explore the relationship and changes among the surface parameters, plasticity index, friction coefficient, contact area ratio, film thickness, and wear scar during the running-in process in order to better understand how the contact surfaces changes during the running-in process.

2. THEORITICAL RUNNING-IN MODEL

Many researchers suggested several contact models between surfaces in the literature. For elastic contact between smooth spherical surfaces, the Hertz model is well-known and widely used [14]. Greenwood and Tipp

extended Hertz model assuming one of the surfaces to be rough in their model [15]. Jeng and colleagues [16] built a model that explains how the surface topography of general surfaces changes during running-in. Horng [17] proposed a micro contact model for rough surfaces where the existence of surface roughness direction takes into account. To study the elasto-plastic interaction between a deformable spherical body and flat rigid body, Kogut et al. [18] created a finite element model. Later Kogut and Etsion developed a multiasperity rough surface model to predict the static friction coefficient [19]. The model for this research based on an elastic-plastic rough flat surface in interaction with a rigid smooth sphere surface is adapted from Li et al. [20] and Khonsari et al. [21]. The contact model for the research is presented in Figure 1 where asperities come into interaction with the rough flat surface as it is loaded against the smooth sphere and carry the load P. The asperities on the contact surfaces can be deformed in an elastic, plastic or elastic-plastic manner and they formed line contact on the surface.

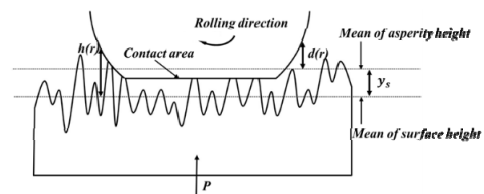


Figure 1. Contact model of a rigid smooth sphere on rough flat surface

2.1 Dimensionless surface roughness parameter

The ratio of standard variation of asperity height and standard deviation of surface height is defined by the dimensionless surface roughness parameter β in the following form [18],

$$\beta = \sqrt{\frac{3.717 \times 10^{-4}}{1 - \left(\frac{\sigma_s}{\sigma}\right)^2}} \quad (1)$$

where β has the form

$$\beta = \eta \rho \sigma \quad (2)$$

2.2 Plasticity index

Plasticity index is an important parameter which was first proposed by Greenwood and Williamson. This parameter is combination of material properties and surface topographical properties. The general plasticity index can be expressed as [18],

$$\psi = \left(\frac{2E}{C_v \pi (1-\nu^2) Y} \right) \left(\frac{\sigma_s}{\rho} \right)^{0.5} \quad (3)$$

2.3 Real contact area ratio

The real contact area of microscopically rough surfaces is an important parameter in the understanding of different tribological phenomena, including wear, fric-

tion, adhesion, frictional heating, contact resistance and etc. Li et al. [20] expressed a fitted dimensional real contact area ratio for sphere on a flat surface which is the ratio of real contact area, and nominal contact area, and has following equation,

$$A_0^* = \frac{A_0}{A_n} = \left(0.47 + 0.57 \exp(-1.2\psi^{0.93}) \right) \left(P^* \right)^{1-0.27 \exp(-1.43\psi^{0.41})} \quad (4)$$

where nominal contact area for this case,

$$A_n = 4BL \quad (5)$$

2.4 Specific film thickness

Predicting film thickness is an important step in developing a lubricated condensed contact and it may provide an easy and fast estimation of film thickness between the lubricated contact surfaces. To determine the stribek curve whether the system can run in a boundary or mixed lubrication regime, the minimum film thickness is used in the measurement of the specific film thickness λ .

$$\lambda = \frac{H_{\min}}{\sigma} = \frac{h_{\min}}{\sigma} \quad (6)$$

where, h_{\min} and σ are minimum film thickness and equivalent surface roughness respectively. Khonsari's [21] proposed central and minimum film thickness equations in his study. Their analytical formula allows rapid prediction of minimum film thickness based on numerical simulations. Film thickness equation contains a wide range of dimensionless tribological parameters and expressed as function of $f(W, U, G, V, \sigma)$, and the dimensionless minimum film thickness is defined in the following form [21],

$$H_{\min} = \frac{h_{\min}}{R} = 1.652W^{-0.077}U^{0.716}G^{0.695} \times \left(1 + 0.026\sigma^{-1.120}V^{-0.185}W^{-0.312}U^{-0.809}G^{-0.977} \right) \quad (7)$$

where, H_{\min} is the dimensionless minimum film thickness and R is equivalent contact radius.

3. TEST APPARATUS AND OPERATING VARIABLES

The running-in experiments were carried out on a disk-on-block tribological test apparatus and schematic view of test machine is shown in Figure 2. The upper disk rotates at a constant speed while the lower block stays stationary in the oil cup. The test apparatus is a combination of many parts including a motor which is attached with bearing through pully and helps to rotate the disk, loading carrier, lubricant cup with block holding facility, and shaft to maintain balancing the disk. The machine is powered by a motor with variable speed. The apparatus is connected with computer by digital instrumentation system which helps to record the

load, speed, temperature and resistance during the run-in time.

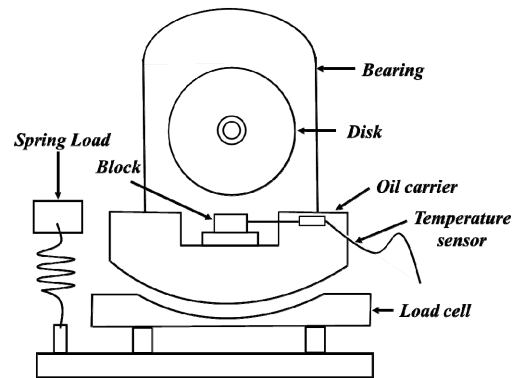


Figure 2. Schematic view of running-in test apparatus

Load, speed, temperature, and resistance sensors are attached with the recorder system to record the data in computer. AISI 1045 steel was used to make the test specimens. The dimension of $(12.5 \times 12.5 \times 12.5)$ mm is used for the block with different surface roughness varies from smooth to very rough $(0.1, 0.3, 0.6) \mu m$ is used for the run-in experiment. Table 1 is lists of the test material properties. The disk had a diameter of 65 mm and a total width of 13 mm and were case-hardened the outer rolling surface that makes it much harder than the block. Hardness is measured by SHIMADZU HMV-G Micro-Vickers Hardness Tester for both test specimens.

Table 1. The properties of the test materials

| Material Properties | Block S45C/AISI 1045 | Disk S45C/AISI 1045 | Units |
|-------------------------|----------------------|---------------------|-------|
| Hardness, Rockwell C | 25.7 | 54.5 | HRC |
| Hardness, Vickers | 270 | 584 | HV |
| Tensile strength, Yield | 490 | 490 | MPa |
| Modulus of Elasticity | 206 | 206 | GPa |
| Poisson's Ratio | 0.3 | 0.3 | - |

Table 2. Physical properties of the lubricant

| Lubricant Properties | R32 | R68 | R100 | Units |
|--------------------------------|-----------------------|-----------------------|-----------------------|------------|
| Fluid density | 0.858 | 0.878 | 0.886 | g/cm^3 |
| Viscosity, Kinematic at 40°C | 31.56 | 67.83 | 100.2 | cSt |
| Viscosity, Dynamic | 0.0271 | 0.0596 | 0.0888 | Pa.s |
| Viscosity, Index | 102 | 98 | 97 | - |
| Pressure viscosity coefficient | 1.98×10^{-8} | 2.31×10^{-8} | 2.48×10^{-8} | Pa^{-1} |
| TAN | 0.17 | 0.19 | 0.18 | $mgKO / g$ |

Three different CPC circulation oils were used as a lubricant for the experiment and the physical properties

of the lubricants shown in Table 2. The lubricants are produced from highly paraffin base oil and anti-rust, anti-oxidation, and anti-foaming additives are included to the lubricants. The oils can produce thick oil films with improved anti-rust, anti-oxidation, and foaming suppression properties. In this experiment, normal load is applied using a spring load cell system attached on the bottom of the oil carrier and connected to digital instrumentation system. The applied load is ranged between 60 N to 100 N and the rolling speed of the disk varied from 100 rpm to 300 rpm (0.17 m/s to 0.51 m/s) for experimental operating condition given in Table 3 and the running in tests is performed for 60 minutes.

Table 3. Operating conditions

| Operating condition | Values | Units |
|---------------------|-----------|---------------|
| Surface roughness | 0.1 ~ 0.6 | μm |
| Applied load | 60 ~ 100 | N |
| Rotating speed | 100 ~ 300 | rpm |
| Time | 60 | min |

4. RESULTS AND DISCUSSION

4.1 Variation in surface topography

According to the mechanism of the disk-on-block test apparatus, the upper specimen is very hard and it is a revolving disk, while the lower block is a fixed square block. As a result, the lower specimen wears out quickly where there is almost no change in the upper disk. The optical micrograph of block surface roughness is shown in the Figure 3, before and after the experiment. On the left side (a, b, c) have different surface roughness from very smooth to very rough before the running in process whereas after the running in process, surfaces of the block is worn out and become more flattened and smoother and it ranged from 0.119 to 0.126 μm .

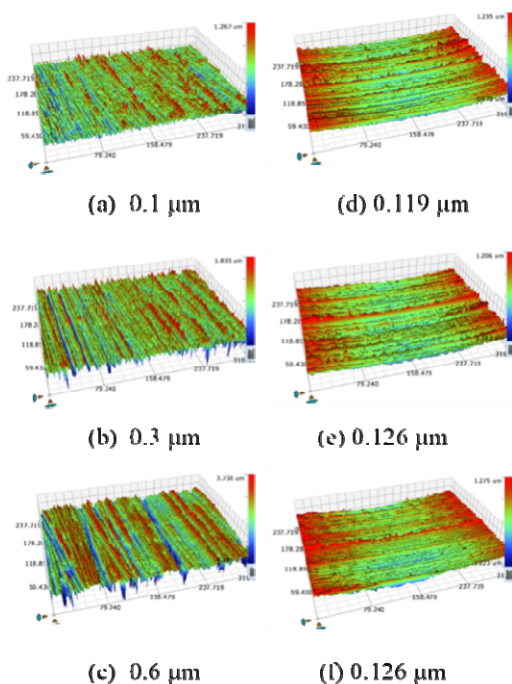


Figure 3. Optical micrographs of block surface roughness before (a, b, c) and after (d, e, f) running-in

The effect of time, load and speed on the root mean square surface heights is investigated in Figure 4. The running-in time has a strong influence on the surface roughness and it decreases as the time is increased as shown in Figure 4(a). The surface roughness R_q value stabilizes after a running-in time and is measured at roughly 0.125 μm . On the other hand, in Figure 4(b) surface roughness is decreased as the load is raised. At the end of the running-in process, surface asperities flattened and surface roughness measured between 0.119 to 0.126 μm . Figure 4(c) shows the fluctuation of surface roughness at different rolling speed and with the increase in the speed surface roughness decreases. Surface roughness recorded high at low rolling speed compared to high rolling speed.

4.2 Variation in dimensionless surface roughness parameter

The variation of dimensionless surface roughness parameter which is the ratio of standard variation of asperity height and standard deviation of surface height for both surfaces, were calculated using equation (1) by analysing the profile data obtained from 3D optical microscope equipped with Vision64 software (Bruker Corporation). The software evaluated those parameters according to which the reference plane was calculated for the Greenwood–Williamson parameters. The variation of dimensionless surface roughness parameter for different load, speed and lubricant is shown in Figure 5. Surface roughness parameter ranged from 0.02 to 0.04, where the values have more variation for different roughness before the running in but after the running in process the difference in the variation is much less because of the surfaces flattened and more asperities removed from the surface.

Figure 5(a) shows the fluctuation of dimensionless surface roughness parameter for different loads before and after the running-in process. Roughness parameter (β) is recorded around 0.33 for lower surface roughness, while it is recorded around 0.25 for the higher surface roughness before the running-in period. After the running-in process, asperities flattened and roughness parameter (β) varies from 0.0306 to 0.0336. However, roughness parameter for different rolling speed is given in Figure 5(b). For various surface roughness under varied speeds, the roughness parameter (β) yielded nearly identical results and it ranged from 0.0254 to 0.0371 before the running-in period and it ranged from 0.0279 to 0.0381 after the running-in. Similarly, in Figure 5(c) for three different lubricants, roughness parameter (β) value varies from 0.0258 to 0.0368 before the running-in period and it measured from 0.0281 to 0.0320 after the running-in process.

4.3 Variation in plasticity index

Variation of plasticity index for different surface roughness which is combination of material properties and surface topographical properties, before and after the experiment is shown in the Figure 6. The plasticity index increases as the surface roughness increases, but after the running-in step, the value is nearly similar because of the

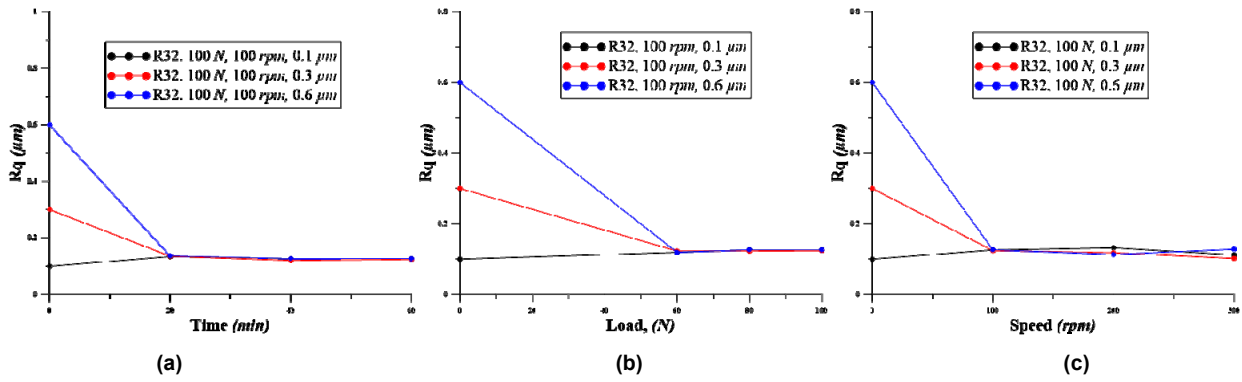


Figure 4. Variation in Rq value for different (a) time (b) load and (c) speed

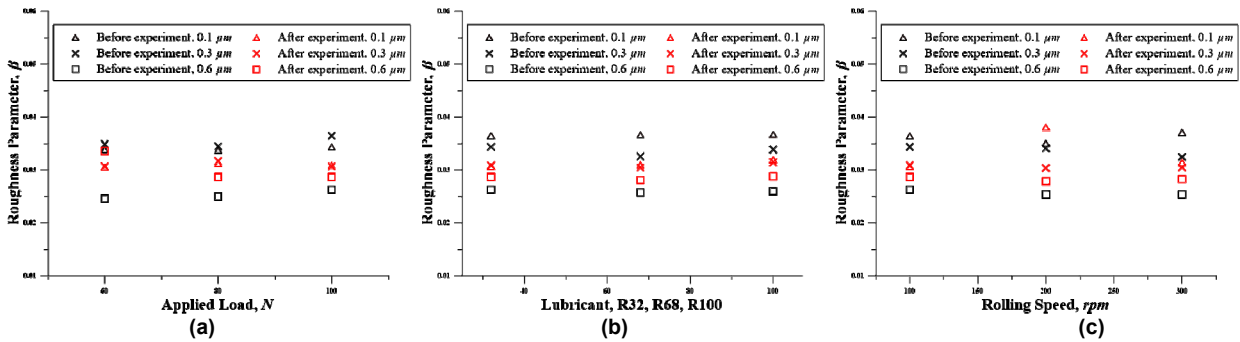


Figure 5. Variation in dimensionless surface roughness parameter for different (a) load (b) lubricant and (c) speed

surfaces smooth out and the asperities flattens. For a very smooth surface, the plasticity index is very low, but as the roughness grows, the plasticity index value increases as well, due to the asperity heights and asperity tip radius of the surface profile. For smooth surface ($R_q = 0.1 \mu\text{m}$), plasticity index recorded as 15.53, while for a rough surface ($R_q = 0.6 \mu\text{m}$), plasticity index recorded as 42.98. But after the running-in process when the asperity gets flattened, the plasticity index value reduced and it ranged from 16.72 to 17.53.

increased as the lubricant viscosity is increased. Plasticity index was recorded lower at low viscosity oil compared to high viscosity oil after the running-in period. For the low viscosity lubricant R32, the plasticity index (ψ) varies from 16.72 to 17.53, while for the high viscosity lubricant R100, it varies from 18.14 to 19.16. The plasticity index values indicate that after the running-in process the $\psi > 10$, which means interaction between neighbouring asperities under fully plastic deformation.

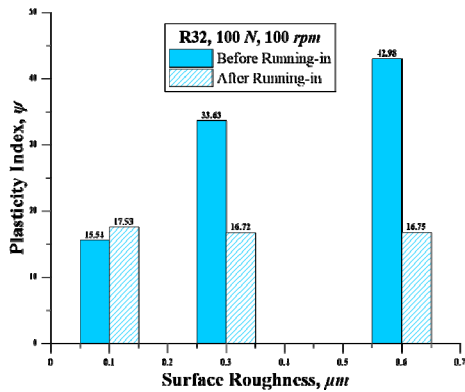


Figure 6. Plasticity index for different surface roughness before and after running-in process

The effect of different load, speed and lubricant on plasticity index is investigated in Figure 7. In the Figure 7(a) the plasticity index is substantially lower when a higher load is applied than when a smaller load is applied because at high load the summits of the surfaces get more flattened. For various surface roughness under varied speeds, the plasticity index yielded nearly identical results as shown in Figure 7(b). However, plasticity index is sensitive to lubricant, as seen in Figure 7(c), and it

4.4 Variation in friction coefficient

The friction coefficient has a significant impact on the investigation of running-in, and it varies depending on the load, speed, and lubrication. Figure 8 shows the recorded friction coefficient over the course of the running-in time for various applied loads, rolling speeds, and lubrications. Because of the asperity to asperity contact between the surfaces, at the starting of the running in process, the friction coefficient is substantially higher, but after a period of running in, the friction coefficient decreases and settles into a steady state condition.

The load has a strong impact on the friction coefficient, Figure 8(a), and it decreases as the load decreases. When a higher load is applied, the friction coefficient is higher than when a smaller load is applied. After the running-in period, the friction coefficient value stabilizes and is measured at roughly 0.025. Figure 8(b) shows the fluctuation of friction coefficient at different rolling speed, while the other parameters such as load, lubricant and time are kept constant. Friction coefficient was recorded high at low rolling speed compared to high rolling speed, and it is recorded around as 0.05 after the running-in.

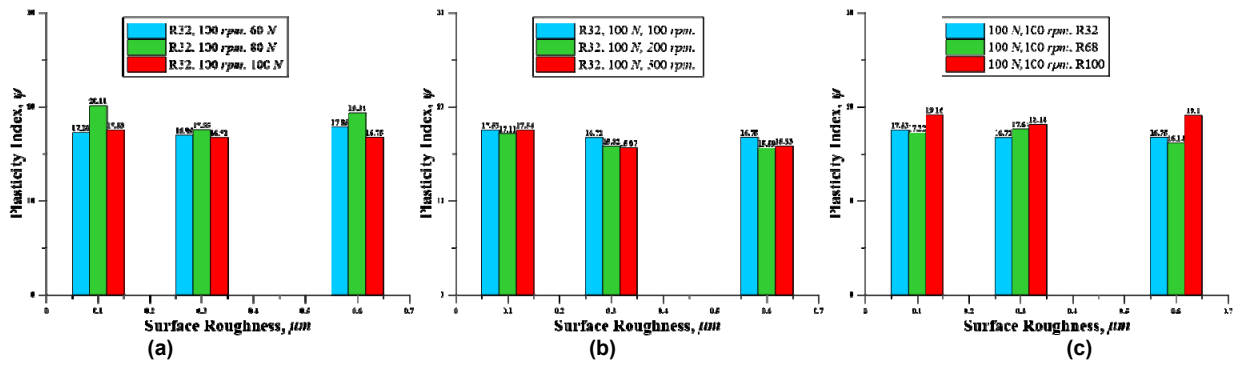


Figure 7. Variation in plasticity index for different (a) load (b) speed and (c) lubricant

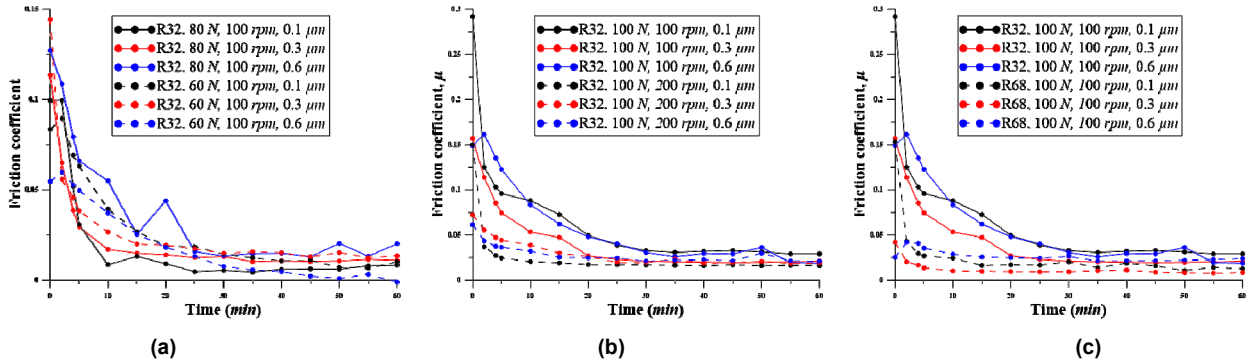


Figure 8. Variation in friction coefficient during running-in for different (a) load (b) speed and (c) lubricant

Friction coefficient is particularly very sensitive to lubricant, as seen in Figure 8(c), and it decreases as the lubricant viscosity is increased. Friction coefficient was recorded high at low viscosity oil compared to high viscosity oil. After a short running-in period, friction coefficient value comes in a stable state and it is recorded less than 0.05 for both the viscosity oils.

4.5 Variation in wear and contact area

After the running in process wear scar is produced on the block surface and the effects of different variables on the surface during running in is evaluated. Figure 9 shows optical micrographs of wear scar after running-in process for different surface roughness under different applied load. On that Figure (a, b, c) are the wear scar micrographs for 60 N applied load, whereas, (d, e, f) are the wear scar micrographs for 80 N applied load. As the load increased the wear scar on the block also increased, for 0.3 μm block at 60 N load, wear scar total length is 5166 μm and width is 1084 μm , whereas, at 80 N load, wear scar total length is 5364 μm and width is 1248 μm .

The effect of applied load, rolling speed and lubrication on nominal contact area after the running-in process is shown in the Figure 10. Although the variance is very tiny for varied surface roughness, it grows progressively as the load increases. The experimental result shows that when the load increases, in the Figure 10(a) the nominal contact area grows rapidly. In comparison to smaller loads, heavier loads have higher and identical nominal contact areas. Figure 10(b) depicts the effect of rolling speed on nominal contact area following the running-in process and it decreased as the speed is increased. Nominal contact area was recorded high at low rolling speed compared to

high rolling speed. At 300 rpm nominal contact area value was recorded smaller and it varies from 4.43×10^{-6} to $5.14 \times 10^{-6} m^2$. Nominal contact area is also very sensitive to lubricant, as seen in Figure 10(c), and it decreases as the lubricant viscosity is increased. Nominal contact area measured high at low viscosity oil compared to high viscosity oil.

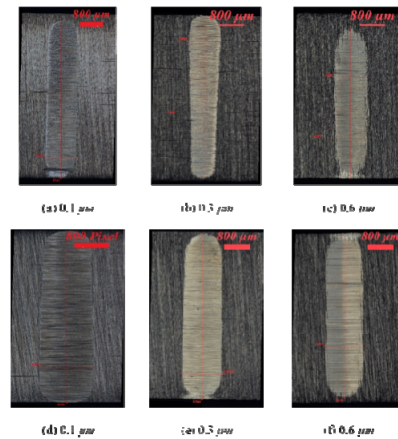


Figure 9. Optical micrographs of wear scar after running-in process for different surface roughness for applied load of 60 N (a, b, c) and 80 N (d, e, f)

The effect of real contact area ratio A_o/A_n after the running-in is shown in Figure 11. The value of contact area ratio is calculated using equation (4). The experimental result shows that in Figure 11(a) when the load increases, the contact area ratio decreases gradually. In comparison to larger loads, lighter loads have high contact area ratio. Figure 11(b) depicts the effect of speed on contact area ratio and it increased as the speed is increased. Contact area ratio was recorded high at low rolling speed compared to high rolling

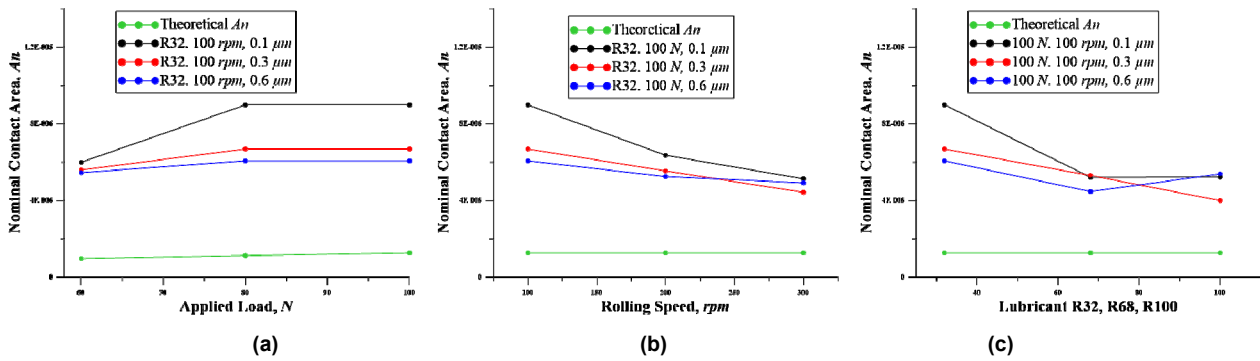


Figure 10. Effect of (a) load (b) speed and (c) lubricant on nominal contact area

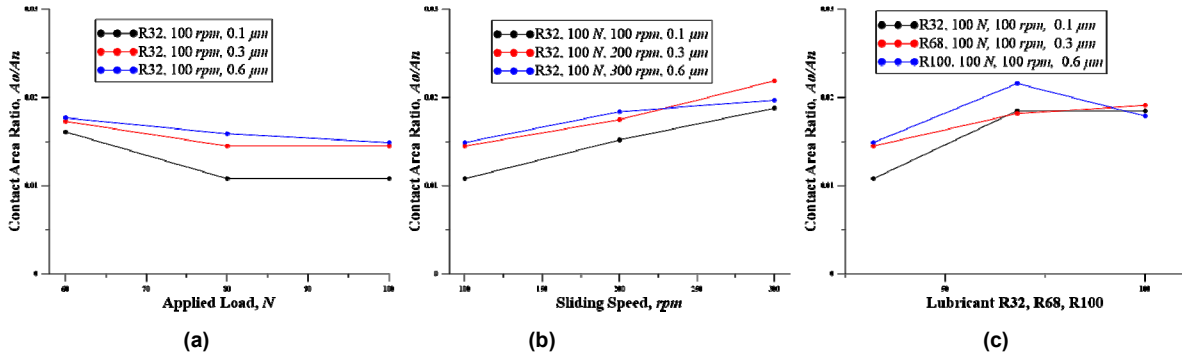


Figure 11. Effect of different (a) load (b) speed and (c) lubricant on contact area ratio

speed. At 300 rpm larger nominal contact area value recorded and it varies from 0.019 to 0.020. The influence of lubrication on contact area ratio is plotted in Figure 11(c), and it increased as the viscosity of the lubricant is increased and contact area ratio measured larger at high viscosity oil compared to low viscosity oil.

4.6 Variation in film thickness

Determining lubrication regimes between contact surfaces is another crucial phase in the running-in process that can help to predict a better run-in outcome. In Figure 12(a), the dimensionless minimum film thickness is plotted against the dimensionless load for different surface roughness values. The load is varied from $W = 1.48 \times 10^{-6}$ to $W = 2.47 \times 10^{-6}$, while the other parameters such as dimensionless speed, dimensionless material number and dimensionless hardness number are kept constant. As shown, the film thickness decreases by increasing the load. Nevertheless, the film thickness is not very sensitive to the variation of load, especially at higher load values ($W = 2.47 \times 10^{-6}$). It is also observed that the dependency of the film thickness on the load is more visible at higher surface roughness values.

As shown, for the smooth surface ($\bar{\sigma} = 9.20 \times 10^{-6}$), the specific film thickness (λ) varies from 1.42 to 1.21 within the given load range, while for the largest surface roughness value ($\bar{\sigma} = 2.11 \times 10^{-5}$), it varies from 1.36 to 1.14. As depicted in Figure 12 (b), film thickness is very sensitive to speed, and it increases by increasing the speed. In fact, increasing the rolling speed changes the lubrication regime. By increasing speed, the specific film thickness λ increases from 1.21 to 1.47 for the

smooth surface ($\bar{\sigma} = 9.20 \times 10^{-6}$), while for the largest roughness ($\bar{\sigma} = 2.11 \times 10^{-5}$), λ changes from 1.14 to 1.20.

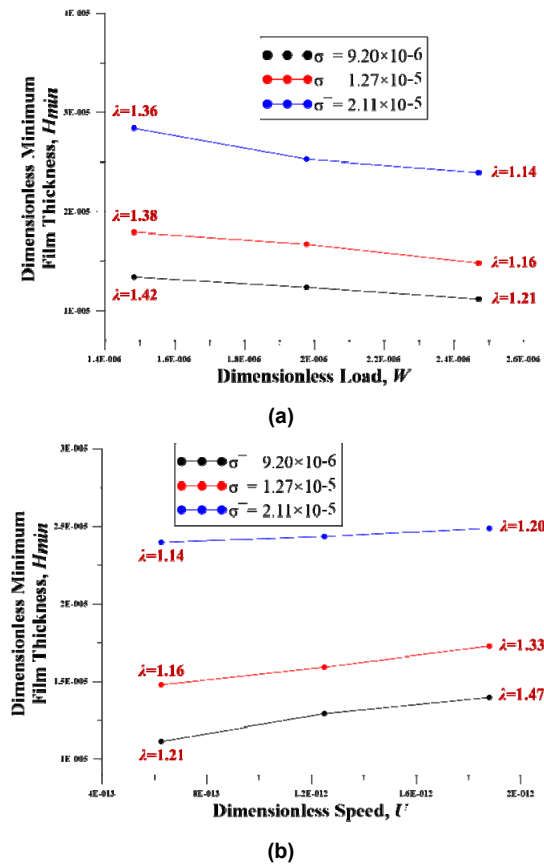


Figure 12. Effect of (a) dimensionless load (b) dimensionless speed on dimensionless minimum film thickness

Figure 13 shows the specific film thickness for different surface roughness under different lubrication, load and speed. For low surface roughness lubrication works under mixed regime whereas the surface roughness increased lubrication regime goes to mixed to boundary regime. As the load increased the specific film thickness decreased. At higher speed thicker film is generated and also lubricant with higher viscosity such as R100 gives thicker film between the surfaces compared to lower viscosity oil R32.

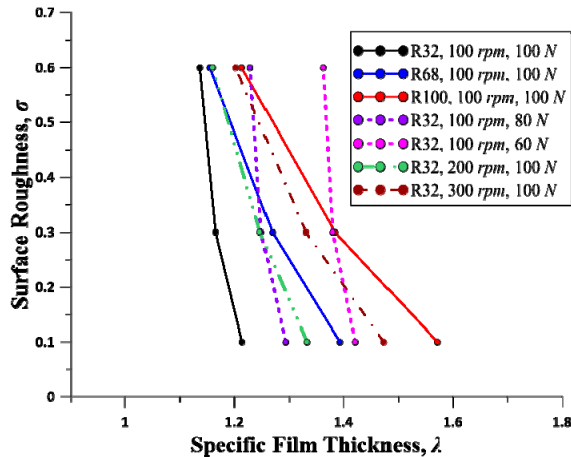


Figure 13. Variation in specific film thickness for different surface roughness under different condition

5. CONCLUSION

The line contact lubricant bath mechanism is used in this study to perform a running-in operating experiment with various loads, speeds, lubricants and roughness values. Theoretical running-in model for a rigid smooth sphere on rough flat surface is discussed and different theoretical parameters are explained based on the running in model. The running in tests is performed and the results are summarized as follows:

- (1) Running-in is primarily impacted by surface topography, and as time passes and varied loads, speeds, and lubricants are used, the surface roughness value steadily decreases and stabilizes.
- (2) The variation of surface roughness parameter before experiment not only range from 0.02 to 0.04, but also from 0.02 to 0.04 after the experiment for different loading because of the asperity parameters.
- (3) The plasticity index rises as the surface roughness rises, but after the running-in process, the value is similar for all surfaces since the surfaces smooth out and the asperity flattens. According to the values of plasticity index, it is shown that the plastic and elastic deformations occur in the running-in process.
- (4) The friction coefficient is recorded higher for rough surfaces than smooth surfaces, although it decreases over the running-in time for all factors and it recorded almost similar values for all different surface roughnesses at the end.
- (5) Theoretically, the nominal contact area is much less, but experimental data reveal significantly greater values, which grow with increasing load

and drop as speed and viscosity increase. The contact area ratio falls as the load increases, but it increases when the speed and viscosity of the lubricant rises.

- (6) As the surface roughness and load decrease, the specific film thickness increases. Higher speeds produce a thicker film, also lubricants with a higher viscosity produce a thicker film between the surfaces.

ACKNOWLEDGMENT

The authors gratefully acknowledges the National Science Council of Taiwan, ROC, which support this research. This paper has been presented at the 10th International Conference on Tribology – BALKANTRIB '20 organised in Belgrade, on May 20-22, 2021.

REFERENCES

- [1] Blau, P. J.: Friction and wear transitions of materials, Noyes, Park Ridge, NJ, 1989.
- [2] Khonsari, M. M.: On the running-in nature of metallic tribo-components: A review, *Wear*, vol. 474-475, pp. 203871, 2021.
- [3] Bhushan, B.: Principles and applications of tribology, Second Edition, Wiley and Sons, New York, 2013.
- [4] Hansen, J., Björling, M., Larsson, R.: Topography transformations due to running-in of rolling-sliding non-conformal contacts, *Tribology International*, vol. 144, pp. 106126, 2019.
- [5] Akbarzadeh, S. and Khonsari, M. M.: Effect of surface pattern on stribeck curve, *Tribol Lett*, vol. 37, pp. 477-486, 2010.
- [6] Zavos, A., Nikolakopoulos, P. G.: Tribological characterization of smooth and artificially textured coated surfaces using block-on-ring tests, *FME Transactions*, vol. 43, pp. 191-197, 2015.
- [7] Horng, J. H.: Contact analysis of rough surfaces under transition conditions in sliding line lubrication, *Wear*, vol. 219(2), pp. 205-212, 1998.
- [8] Wang, W. et al.: Experimental study of the real time in surface roughness during running-in for PEHL contacts, *Wear* 244, pp. 140 - 146, 2000.
- [9] Vite-Torres, J., Vite-Torres, M., Aguilar-Osorio, R., and Reyes-Astivia, J. E.: Tribological and corrosion properties of nickel coatings on carbon steel, *FME Transactions*, vol. 43, pp. 206-210, 2015.
- [10] Sipcikoglu, B. I., Yugit, B., Oflaz, H., Parlar, Z., and Temiz, V.: The investigation of friction and wear characteristic of cast iron against manganese phosphate coated and austempered compressor crankshaft, *FME Transactions*, vol. 43, pp. 186-190, 2015.
- [11] Chern S. Y., Ta, T. N., Horng, J. H. and Wu, Y. S.: Wear and vibration behavior of ZDDP-Containing oil considering scuffing failure, *Wear*, vil. 478-479, pp. 203923, 2021.

- [12] Ziegler, A., Emrich, S., Lohner, T., Michaelis, K., Brodyanski, A., Merz, R., Stahl, K.: Influence of tribofilms on failures and friction of gears with particular focus on running-in. *Industrial Lubrication and Tribology*, vol. 71(8), pp.1017-1026, 2019.
- [13] Dowson, D., Higginson, G. R.: *Elasto-hydrodynamic lubrication*, Pergamon Press, London, 1977.
- [14] Hertz, H.: On the contact of elastic solids, In: *Miscellaneous Papers*, Chapter V, pp.146-162. by Hertz, H. and Lenard P., translated by Jones, D. E. and Schott G.A., London: Macmillan, 1896.
- [15] Greenwood, J. A. and Tripp, J. H.: The elastic contact of rough spheres, *ASME. J. Appl. Mech.*, vol. 34(1), pp.153–159, 1967.
- [16] Jeng, Y. R., Lin, Z. W. and Shyu, S. H.: Changes of surface topography during running-in process, *ASME-Journal of Tribology*, vol. 126, pp. 620-625, 2004.
- [17] Horng, J. H.: An elliptic elastic-plastic asperity microcontact model for rough surfaces, *ASME. J. Tribol.*, vol. 120(1), pp. 82–88, 1998.
- [18] Kogut, L. and Etsion, I.: A finite element based elastic-plastic model for the contact of rough surfaces, *Tribology Transactions*, vol. 46(3), pp. 383–390, 2003.
- [19] Kogut, L. and Etsion, I.: A static friction model for elastic-plastic contacting rough surfaces, *ASME. J. Tribol.*, vol. 126(1), pp. 34–40, 2004.
- [20] Li, L., Etsion, I. and Talke, F. E.: Contact area and static friction of rough surfaces with high plasticity index, *ASME. J. Tribol.*, vol. 132(3), pp. 031401, 2010.
- [21] Masjedi, M. Khonsari, M. M.: Film thickness and asperity load formulas for line-contact elastohydrodynamic lubrication with provision for surface roughness, *ASME Journal of Tribology*, vol. 134(1), pp. 011503, 2012.

NOMENCLATURE

| | |
|---------|---|
| A_0 | real contact area |
| A_n | nominal contact area |
| A_0^* | real contact area ratio |
| β | dimensionless surface roughness parameter |
| B | contact width |
| C_ν | function of poisson's ratio |

| | |
|----------------|--|
| E | young's modulus |
| η | area density of asperity |
| ψ | plasticity index |
| λ | specific film thickness |
| G | dimensionless material number |
| H_{\min} | dimensionless minimum film thickness |
| h_{\min} | minimum film thickness |
| L | contact length |
| σ | standard deviation of surface heights |
| σ_s | standard deviation of asperity heights |
| $\bar{\sigma}$ | dimensionless surface roughness |
| ρ | asperity tip radius of curvature |
| P^* | dimensionless normal load |
| R | equivalent contact radius |
| R_q | root-mean-square roughness |
| U | dimensionless speed number |
| V | dimensionless hardness number |
| ν | poisson's ratio |
| W | dimensionless load number |
| Y | yield strength |

ИСТРАЖИВАЊЕ ПРОЦЕСА УХОДАВАЊА БАЗИРАНОГ НА ПАРАМЕТРИМА ХРАПАВОСТИ ПОВРШИНЕ, ОДНОСУ СТВАРНИХ КОНТАКТНИХ ПОВРШИНА И ТРИБОЛОШКИМ СВОЈСТВИМА

J.Х. Хорнг, Д. Бисвас, Адхитја, К. Ахсан

Процес уходавања представља процес у коме покретни делови почињу да се тару један о други како би се успоставило прилагођавање облика у стабилан однос за преостали део њиховог радног века. Циљ рада је истраживање и евалуација процеса уходавања коришћењем уређаја за контакт са диском на блоку. Разматра се микро-контактни модел асперитета израђен на основу искуства и темељне анализе. Експеримент је изведен варирањем храпавости површине блока круте глатке површине сфере у одређеним условима. Истражен је утицај храпавости површине, оптерећења, брзине и подмазивања на процес уходавања. Уходавање изазива пластичну деформацију асперитета и микроструктурне промене на контактним површинама. Теоријски и експериментални резултати показују да процес уходавања има утицаја на индекс пластичности ψ , параметар површинске храпавости β , однос стварних контактних површина A_0^* и дебљину филма λ .